Comparison of the results of numerical and geometrical outdoor acoustic simulations in a real-life area

Kazuma HOSHI[1]; Takuya OSHIMA[2]; Yasuhiro HIRAGURI[3]

[1] Dept. of Architecture and Living Design, Junior College, Nihon University, Japan

[2] Faculty of Engineering Niigata University, Japan

[3] Dept. of Civil Eng. and Architecture, National Institute of Tech., Tokuyama College Japan

ABSTRACT

Authors are developing a real-life outdoor finite-difference time-domain (FDTD) acoustic simulation using land cover acoustic characteristics. On Inter-noise 2012 and 2013, the identification method of land surface from airborne hyperspectral imagery was presented. Additionally, the identified surface characteristics are given to finite-difference time-domain outdoor acoustic simulations in a real-life area and the calculation results was reported. In present study, the calculation results of previous report are compared with that of using geometrical acoustic simulation.

Keywords: Real-life outdoor finite-difference time-domain (FDTD) acoustic simulations, Real-file outdoor Geometrical acoustic simulations, Land cover acoustic characteristics, Airborne hyperspectral imagery

1. INTRODUCTION

Wave equation based acoustic simulation techniques have been being developed rapidly in recent years. These techniques, however, have not been yet applied to urban noise prediction. That is because a target area is generally too large and the land surface data and topographical data are too difficult to obtain it as reasonable format for the wave based simulations. For making a break through to the next stage, authors are developing a real-life outdoor finite-difference time-domain (FDTD) acoustic simulation using land cover acoustic characteristics from 2011. On Inter-noise 2012 and 2013, the identification method of land surface from airborne hyperspectral imagery was presented [1, 2]. Additionally, the identified surface characteristics are given to finite-difference time-domain outdoor acoustic simulations in a real-life area, and the calculation results ware reported [3]. The purpose of this paper is comparison of the calculation results using geometrical simulation with that of using numerical one reported previous paper.

2. OUTLINE OF IDENTIFICATION OF LAND SURFACE [2]

2.1 Hyperspectral imagery

Figure 1(a) presents hyperspectral imaging data for Nagaoka, Niigata, in a RGB mode. The image was obtained by PASCO Corp. on 5 June 2004 using the Airborne Imaging Spectroradiometer for Application (AISA), which is a hyperspectral sensor with a 1 m spatial resolution developed by Spectral Imaging Ltd. The image data comprise 67 bands, covering both the visible and a part of near-infrared wavelengths from 400nm to 1000 nm. Spectral bands width is equally spaced by 8 or 9 nm.

2.2 Land cover category

The land cover category that should be estimated is determined by referring to ASJ RTN-Model 2008 [4] in the first step to discuss classification methods. ASJ RTN-Model 2008 defines land cover classifications of four categories: loose soil (soft farmland and furrowed rice fields), grassland (lawn, rice fields, and grassland), compacted soil, and concrete and asphalt. The corresponding effective flow resistivities are, respectively, 75, 300, 1,250 and 20,000 $kPas/m^2$. In this report, the land cover classification that must be estimated is decided from five categories (Table 1).

---

[1] hoshi@arch.jcn.nihon-u.ac.jp

[2] oshima@eng.niigata.ac.jp

[3] hiraguri@tokuyama.ac.jp
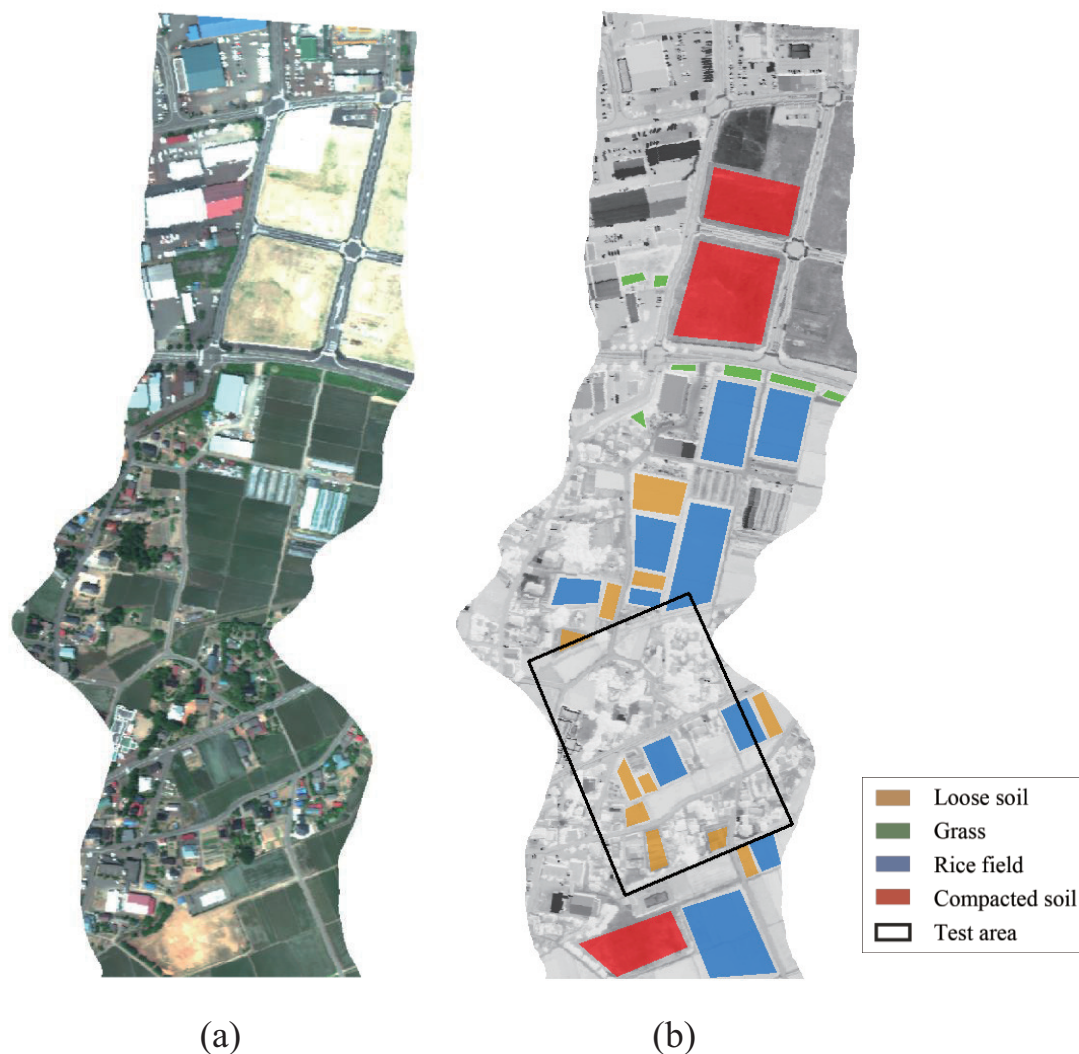
(a)   (b)

Figure 1 – (a) Hyper-spectral imaging data measured in Nagaoka, Niigata in RGB mode, (b) Training and test area for estimating land cover classification.

Table 1 – Flow resistivity for each land cover class used for classification.

Land cover category	Effective flow resistivity [kPa s/m^2]
Loose soil	75
Grass	300
Rice field	300
Compacted soil	1,250
Others	20,000

2.3   Identification method of category

MED-SD method which is used in this study, for classifying land cover categories using hyperspectral imaging data, combining the characteristics of MED method [5] and SD method [6]. The MED-SD method normalizes each value calculated from the MED method and the SD method. Some training areas were set as in Fig. 1(b) to decide the averaged spectrum of each absorption land cover categories.

2.4   Result of identification

In order to confirm the discriminant accuracy of MED-SD method, the land cover categories are estimated at the test area surrounded by the black line in Fig. 1(b). The identification result used in this study is the one reported in Ref. [7]. The threshold of 95 percentile used in the identification is same as the value used in the Inter-Noise 2012 paper [1], but a revised classification algorithm is used. The optimal threshold of 85
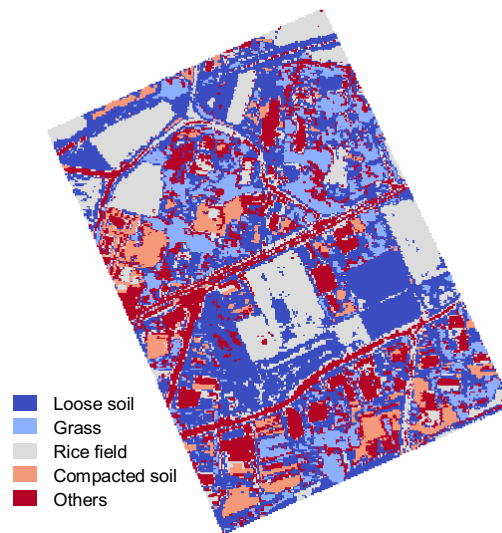
Figure 2 – Land category estimation result with 95 percentile threshold.

percentile later found in the Inter-Noise 2013 paper [2] is not applied. However, the use of the non-optimal classification result should not essentially affect the results of this study. The result of identification is shown in Figure 2. In this report, this classified data is used for numerical and geometrical simulation.

3.   NOISE LEVEL PREDICTIONS IN REAL-LIFE AREA USING NUMERICAL AND GEOMERTICAL ACOUSTIC SIMULATIONS

3.1   Configulation of calculation using numerical method [3]

The real-life subject used in the study is an area of $210[\text{m}] \times 290[\text{m}]$ in x and y directions in Nagaoka, Japan shown in Figure 3 (same area shown in Figure 2). The terrain and building geometries are reconstructed by the technique developed in a former study [8] using a digital surface model [9] and a building outline dataset [10]. The height of the computational domain is 50 m (including the height of the ground portion of about 1 m). The grid spacing is 0.125 m. With the given grid spacing, the number of grid points are $1680 \times 2320 \times 344$ (for $x \times y \times z$ directions shown in Figure 3). The lateral and the upper domain bounds are additionally enclosed by a PML of 20 grids thickness. 167 point sources are placed with a 1.25 m interval from $x = 1.25[\text{m}]$ to $x = 207.75[\text{m}]$ along the source line in Figure 3 at 0.3 m above ground level assuming a road traffic noise source. The sources are covered up to 250 Hz octave band. The receivers are located at R1 to R6 in Figure 3 with the height above the ground of 1.5 m. Time integration step is 2×10^4 s. The end time is 2 s. The detail of calculation about how to include the land surface classification is described in previous study[3].

For contrasting purpose, a case with the same geometry but with rigid surfaces (case R), and a free field case with the same domain size but with an additional PML at the lower domain bound (case F) are also solved.
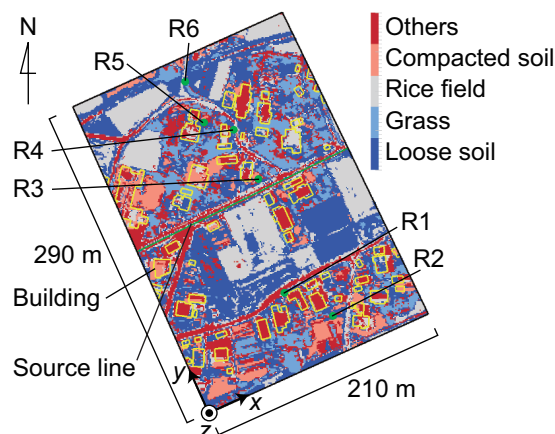

Figure 3 – Subject area.

3.2   Configulation of calculation using geometrical acoustic simulation

The test area is same as used in the numerical calculation. The terrain and building geometries are directly set a digital surface model [9] and a building outline dataset [10]. The land classification data shown in Figure 3 is also same as used in the numerical calculation. The source and receive points are also set as same locations as used in the numerical calculation. There are 167 source points lined 1.25 m interval and 0.3 m above the road. The six receiving points are set at 1.5 m height. There are shown in Figure 3. For geometrical simulation, Harmonoise [11] is selected. Harmoniose is developed by official institutes and is semi-open-source ware, so that it is easy to use for authors. How to make dataset to calculate before passing to Harmonoise is as follows:

1) Read the geometry and land classification data.
2) Obtain the section data by slicing the plane which includes the combination of selected a source point and a receiving point. Figure 4 (a) shows the topographical data and the slicing plane. Figure 4 (b) shows the cross section contour.
3) Select the sound traveling segment from the contour line. The segment is between the source and the receiving point. Figure 4 (c) shows the selected segment from the cross section contour.
4) Supply the land classification data to each section data points. The coordinate of a point of cross section are checked against the coordinate of land surface data, and the land category data of the nearest point is picked out.
5) Pass the data of distance from the source point and that of land category at each point in this segment to Harmonoise

Harmonoise returns the levels from one source point to one receiving point. Therefore, to obtain a level at one receiving point, the energies arrived from 167 sources are composed. After that, 1/3 ocave band levels form 25 Hz to 10 000 Hz are obtained. These values are composed to obtain 1/1 octave band level for comparison. To confirm the calculation results of both method, three cases are set. First one is free field (No land terrain and classification data) (it is called Case F). Second one is all rigid land terrain (Case R). Third one is using land terrain and classification data (Case A). These cases are same as that of numerical calculation.
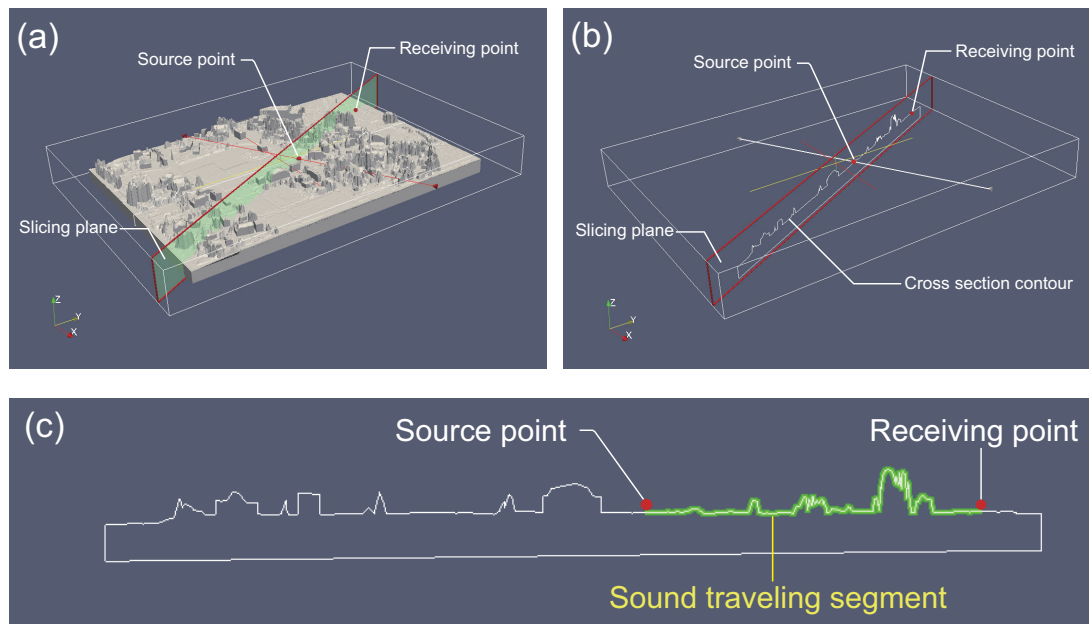

Figure 4 – Procedure of obtaining the topographical data from a source and a receiving point.

Table 2 – Flow resistivity for each land cover classification for the calculation with Harmonoise.

Land cover category	Effective flow resistivity [kPa s/m^2]
Loose soil	80
Grass	200
Rice field	200
Compacted soil	2,000
Others	20,000

3.3   Comparison of numerical calculation results and geometrical ones

Figure 5 shows the calculation results using numerical method[2]. The results are represented as octave-band sound pressure level differences of case R relative to case F (ΔL_{RF}), case A relative to case F (ΔL_{AF}) and case A relative to case R (ΔL_{AR}). At receiver R1 where sound propagates over a rice field without being shielded by buildings, ΔL_{RF} is positive due to reflections by the ground and by the buildings behind the receiver. However, 7 dB of attenuation is observed for ΔL_{AF} with regard to ΔL_{RF} at the same receiver for a frequency of 250 Hz. The difference demonstrates the effects of the porous property of the surfaces. At receiver R2 which locates behind a building, both ΔL_{RF} and ΔL_{AF} attenuate with increasing frequency due to shielding by the building, with additional ground absorption in case of ΔL_{AF}.

Figure 6 shows the calculation results using Harmonoise. Relative sound pressure level differences (ΔL_{RF},
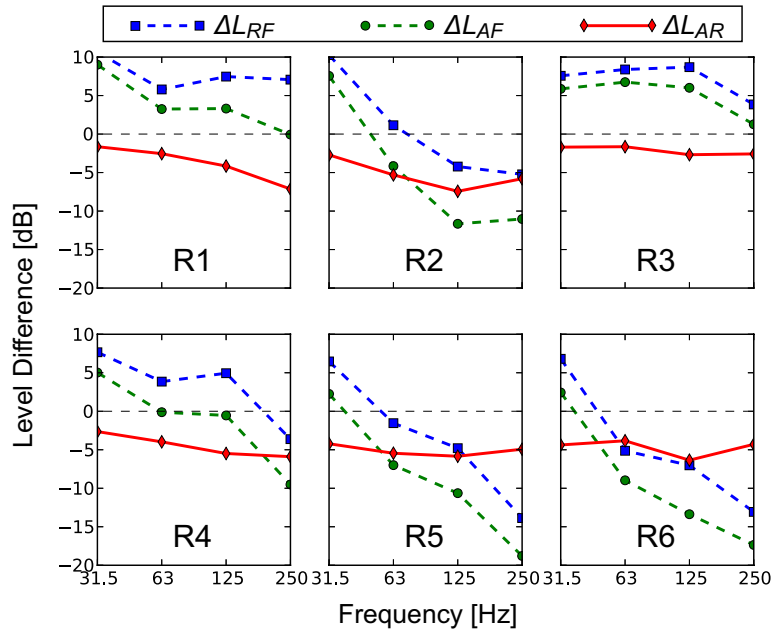

Figure 5 – The calculation results using FDTD method. Octave-band relative sound pressure levels obtained at R1 – R6.
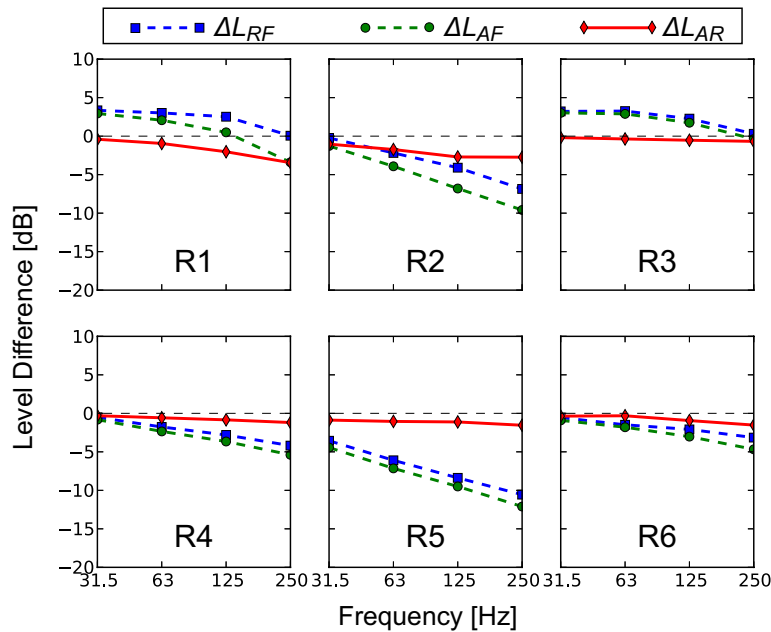

Figure 6 – The calculation results using Harmonoise. Octave-band relative sound pressure levels obtained at R1 – R6.

ΔL_{AF}, ΔL_{AR}) represent same as the results using numerical method shown in Figure 5. At first, focusing on the tendency of attenuation level at each receiving point, it can be seen that the results of using Harmonoise shown in Figure 6 resemble the result of using numerical method shown in Figure 5. However, the results of using Harmonoise are smaller than using numerical method at each receiver point. At receiver R1, focused on ΔL_{AF} (green dotted line), the higher frequency, the more sound level is attenuated more than the result rigid surface(ΔL_{RF}: blue dotted line), it caused by the influence of the land surface. The attenuation level at receiver R2 is more than that at receiver R1. This phenomenon is caused by the influence of land surface and insulation of buildings. These tendencies are shown in the results of using FDTD method in Figure 5. At other receiving points, the tendency of attenuation calculated using numerical method also resembles that of Harmonoise.

From this study, we can see that the noise propagation simulation using numerical calculaiton with land surface classification data is fairly trustworthy.

4. CONCLUSION

In the present study, our proposed method (identified surface characteristics of a real-life area by airborne hyperspectral imagery given to a finite-difference time-domain outdoor acoustic simulation) is compared with geometrical acoustic simulation using Harmonoise. The results of this study shows us that the numerical simulation in real-life area might be trustworthy method.

ACKNOWLEDGEMENTS

REFERENCES

[1] Yasuhiro Hiraguri, Takuya Oshima, and Kazuma Hoshi. Case study of land cover classification estimation using hyperspectral imaging data for outdoor acoustic simulations. *In Proc. Inter-Noise 2012 (New York) in CD-ROM*, 2012.

[2] Yasuhiro Hiraguri, Takuya Oshima, and Kazuma Hoshi. Improvement of estimation method of land cover acoustic characteristics using hyperspectral imaging data. *In Proc. Inter-Noise 2013 (Innsbruck) in CD-ROM*, 2013.

[3] Takuya Oshima, Yasuhiro Hiraguri, and Kazuma Hoshi. Finite-difference time-domain outdoor acoustic simulation of a real-life area using land cover acoustic characteristics identified by airborne hyperspectral imagery. *In Proc. Inter-Noise 2013 (Innsbruck) in CD-ROM*, 2013.

[4] Kohei Yamamoto. Road traffic noise prediction model "asj rtn-model 2008": Report of the research committee on road traffic noise. *Acoustical Science and Technology*, 31(1):2–55, 2013.

[5] N. Keshava. Distance metrics and band selection in hyperspectral processing with applications to material identification and spectral libraries. *Geoscience and Remote Sensing*, 42:1552–1565, 2004.

[6] M. A. Cochrane. Using vegetation reflectance variability for species level classification of hyperspectral data. *International Journal of Remote Sensing*, 21(10):2075–2087, 2000.

[7] Yasuhiro Hiraguri, Takuya Oshima, and Kazuma Hoshi. Basic investigation on estimation of land cover classification conforming to the asj rtn-model using hyperspectral imaging data. *Acoustical Science and Technology*, 34(1):367–370, 2013.

[8] Takuya Oshima, Yasuhiro Hiraguri, and Masashi Imano. Geometry reconstruction and mesh generation techniques for acoustic simulations over real-life urban areas using digital geographic information. *Acoustical Science and Technology*, 35(2):108–118, 2014.

[9] Ltd Kokusai Kogyo Co. Rams-e surface level 1. `http://www.ramse3d.com/laser/lib/index.html`.

[10] Geospatial Information Authority of Japan. Fundamental geospatial data (accuracy level 2500). `http://www.gsi.go.jp/kiban/index.html`.

[11] Renez Nota, Robert Barelds, and Dirk van Maercke. Harmonoise WP 3 Engineering method for road traffic and railway noise after validation and fine-tuning. Technical Report - Delverable 18, January 2005. HAR32TR-040922-DGMR20.